ELSEVIER

Nuclear Instruments and Methods in Physics Research B 144 (1998) 246–255

NIM B
Beam Interactions with Materials & Atoms

Imaging single living cells with a scanning near-field infrared microscope based on a free electron laser

M.K. Hong [a], A.G. Jeung [b], N.V. Dokholyan [a], T.I. Smith [b], H.A. Schwettman [b], P. Huie [c], S. Erramilli [a,*]

[a] *Physics Department and the Center for Photonics, Boston University, MA, USA*
[b] *Hansen Experimental Physics Laboratory, Stanford University, Stanford, USA*
[c] *Department of Pathology, Stanford University Medical School, Stanford, USA*

Abstract

We report the first sub-wavelength mid-infrared images under water, and describe an application to obtaining images of single living cells in water using the Stanford Free Electron Laser (FEL). Spatial resolution is enhanced at the peak of infrared absorption of water. Images were obtained of single motile fibroblasts with the FEL wavelength tuned to absorption peaks of both protein and lipid molecules. Analysis of the unexpectedly strong absorption due to lipid molecules in motile fibroblasts suggests that the concentration of lipid molecules in lamellopodia is consistent with membrane flow.

PACS: 87.64t; 41.60Cr; 87.64Je; 87.15Mi

1. Introduction

Infrared spectroscopy is one of the most sensitive techniques for the analysis of biological systems. Many biomolecules like lipids, proteins and nucleic acids have normal modes that are infrared active [1]. These normal modes are so characteristic that the region of the spectrum between 4 and 12 μm is often called the "fingerprint" region (see Fig. 1). A combination of infrared spectroscopy and microscopy provides a new tool for non-destructive characterization of samples, and for localization of specific molecules within a sample [2,3]. The ability to localize specific molecules or molecular groups is useful in a wide range of problems in biological physics. The absorption cross-sections associated with many vibrational modes are sufficiently high (between 10^{-19}–10^{-16} cm^2) that it is possible to identify the presence of specific molecules at the sub-picogram level without having to use fluorescent stains or radioactive labels. Recognition of this sensitivity has led to the commercial development of Fourier transform infrared spectrometers (FTIR) attached to infrared microscopes as a powerful method for microanalysis in biomedical applications. These

* Corresponding author. Address: 590 Commonwealth Avenue, Boston, MA 02215, USA. Tel.: 617 353 1271; fax: 617 353 9393; e-mail: shyam@bu.edu.

0168-583X/98/$ – see front matter
PII: S0168-583X(98)00311-5

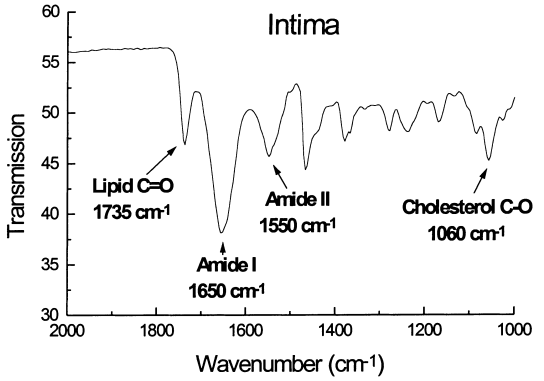

Fig. 1. An infrared spectrum of a cross-section of artherosclerotic tissue, showing absorption bands due to the presence of ester-linked acyl chains in lipid, amide bands in proteins, and cholesterol [3]. The absorption lines serve as a "fingerprint" for localizing molecules.

microscopes use Cassegrainian objectives, which have reduced numerical apertures (generally 0.6 or less) compared to refractive objectives, but have the advantage that the focal length is the same throughout the infrared region of the spectrum. Spectra are usually collected from a small (~25 μm × 25 μm × 5 μm) region of a dehydrated sample placed on an infrared microscope stage. The relatively small numerical apertures, combined with the low brightness of the broadband Globar source (~1200 K) used limits the spatial resolution to roughly 25 μm, well above the diffraction limit. With the recent development of an infrared beamline at the synchrotron light source at Brookhaven, Carr et al. have demonstrated that it is possible to reach the diffraction limit in infrared microscopy [4]. Images may be acquired by raster scanning a sample beneath the focussed broadband infrared beam collecting a spectrum at each pixel [5]. At a rate of several minutes for each pixel, acquisition of a 100 × 100 pixel image of a sample is time consuming. Infrared microspectrometers coupled to infrared focal plane array detectors allow for parallel acquisition of spectra from every pixel in the image [6]. Because of the optics and the low brightness of the Globar sources used, the spatial resolution of this method has not reached the diffraction limit, even on dehydrated samples.

When water is added, the strong absorption throughout the infrared region of the spectrum (see Fig. 2) makes both spectrum and image acquisition in the infrared region very difficult. The attenuation length for liquid water in this wavelength range is so short (~0.8–10 μm) that in order to be able to obtain images, the imaging optics have to be positioned extremely close to the surface of the sample. Conventional far field imaging techniques using optical elements like lenses are difficult with such short path lengths. The difficulties are acute enough that, until this year there have been no published infrared images under water in this spectral range.

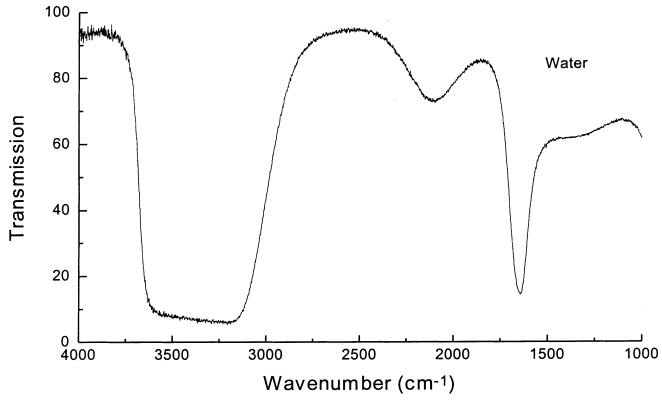

Fig. 2. Infrared spectrum of liquid water. The relative transmission (arb. units) is shown as a function of frequency. The strong absorption near 1600 cm^{-1} coincides with the amide band region.

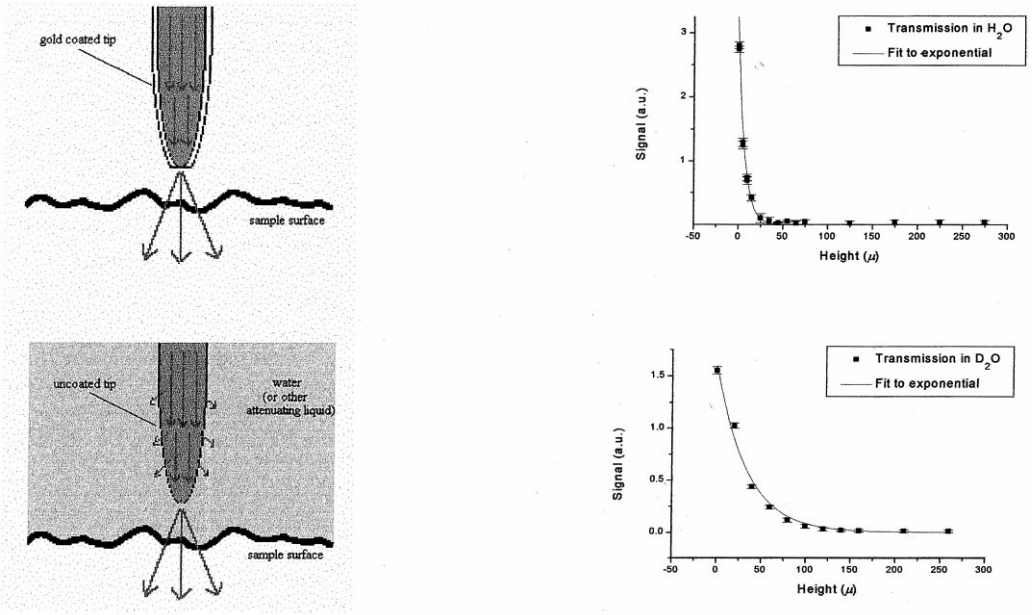

Fig. 3. (Left) Schematic picture of the essential idea for obtaining underwater infrared images. (Right) Normalized transmitted signal at an FEL wavelength of 6.05 μm, through a tapered SNIM probe as a function of the separation between the probe and the surface of the substrate, immersed in liquid water and D_2O. The range of separation over which a signal can be detected is about 6 μm in H_2O compared to about 30 μm in D_2O, consistent with the absorption cross-sections of the two liquids at this wavelength.

A solution to the problem of short path lengths is to position the source of light extremely close to the sample in order to reduce the effects of absorption in the surrounding medium, as illustrated in Fig. 3 [7]. Infrared radiation from the Stanford Free Electron Laser (FEL) is coupled to one end of a chalcogenide fiber. The other end of the fiber is tapered to form a sub-wavelength aperture. The sample is placed on a CaF_2 window in the near-field of infrared radiation transmitted by the tapered fiber [8,9]. The transmitted signal is detected using infrared optics positioned below the substrate [10]. The sample is scanned using piezoelectric transducers, and images are obtained one pixel at a time. The technique is called Scanning Near-field Infrared Microscopy (SNIM), an extension to the infrared region of scanning near-field optical microscopy (SNOM [11] or NSOM [12]) under water [13]. Here we show that the problem of underwater infrared imaging can be overcome with scanning probe techniques.

2. Methods

One feature of the near-field technique is that the tapered end of the fiber is less than the cut-off wavelength. SNIM probes have very low transmission factors, in the range 10^{-4}–10^{-6}. Attempting to overcome the small transmission factor by using high laser power, such as that provided by the Stanford FEL, is not possible for imaging in air or vacuum because of thermal damage to the end of the fiber. In conventional SNOM, in the visible region of the spectrum, the laser power is usually kept below about 10 mW in order to avoid destruction of the gold coating on the tapered end of the fiber. Immersion of the tapered fiber in liquid water allows us to use the full 2 W power of the Stanford FEL without destroying the tip. For routine imaging studies, and for initial alignment, a small portion (~10%) of the FEL beam was picked off using a beam splitter and used for SNIM. The SNIM could thus be operated in

parasitic mode for extended periods. For underwater imaging of single living cells, the beam splitter was replaced by a mirror, and the full power of the FEL beam was available for near-field imaging. The laser power emerging from the tip into the water was estimated to be about 2 μW. The temperature rise, measured by using a fluorescent marker, is less than 2 K [14]. The use of high laser power allows for faster data acquisition, limited only by the response of the positioning stage (15 Hz with feedback, 10 kHz without feedback) with a signal-to-noise ratio of about 3%. Because of the pulse structure of the FEL source used, the sample stage used for scanning has to be synchronized [9] to the Stanford FEL pulses, which occur in macropulses that last 3 ms at a 20 Hz repetition rate. Each macropulse consists of ~1 ps duration micropulses, repeating at 11.8 MHz [15]. A comparison of various sources of infrared radiation for SNIM is shown in Fig. 4.

As the distance between the tip and sample is decreased, the signal increases exponentially (Fig. 3). Furthermore, when the signal was measured through both H_2O and D_2O at an FEL wavelength of 6.05 μm one can see a significant difference in the decay lengths due to the different attenuation lengths for the two liquids. Spatial resolution was determined by depositing a thin (~80 nm) film of Chromium on a calcium fluoride substrate. The thickness of the metal film was measured with an Atomic Force Microscope [16]. Fig. 5 shows a sequence of images obtained at varying heights. The spatial resolution in near-field microscopy degrades as the tip-sample distance is increased, with the best spatial resolution achieved under water being $\lambda/3$. When uncoated tips or tips with damaged coating are used, spatial resolution is also degraded because the signal collected is emitted not just from the aperture at the end, but from points higher up on the probe. The presence of an absorbing medium like water prevents signal leaking from higher up the tip from reaching the detector. It is therefore possible to obtain high resolution infrared images from tapered probes that are not coated at all. This is particularly useful for biological systems where the metal on the tip can affect living cells. Fig. 5 shows that a resolution of 2 μm was obtained at a wavelength of 7.47 μm. Fig. 5 also shows that spatial resolution is lost when water is removed, but is restored when water is reintroduced. One interesting consequence of using uncoated tips is that the spatial resolution is expected to be highest at the wavelengths that are strongly absorbed by the surrounding medium. Fig. 6 shows an underwater image at two different wavelengths of a pattern of gold lithographed onto a silicon substrate. An image was first obtained at 6.25 μm, close to an absorption peak in liquid

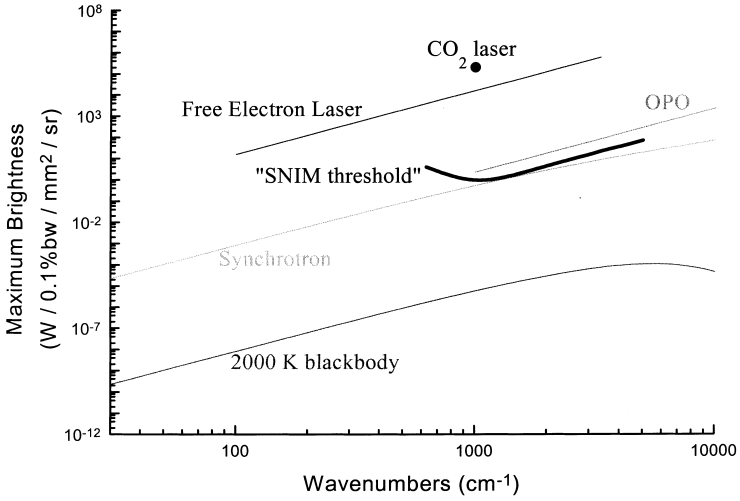

Fig. 4. Comparison of various infrared sources for SNIM, using measured values of transmission losses in the tapered SNIM probes.

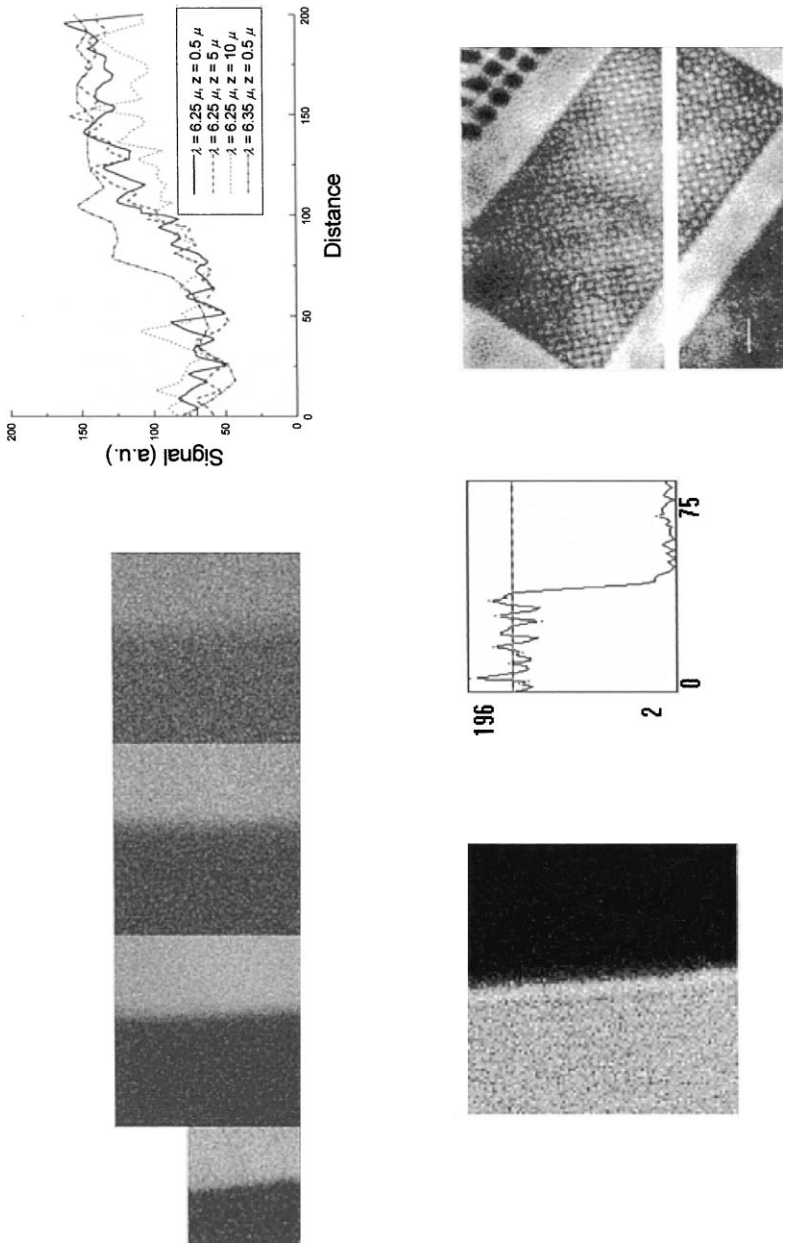

Fig. 5. (Top): Sequence of images of an edge formed by a 120 nm gold layer on a silicon substrate, imaged in transmission in water, at varying probe heights z. (Bottom Left): Underwater image at a wavelength of 7.47 μm, of an 80 nm chromium edge on a CaF_2 substrate. (Bottom Center): Analysis of the transmitted signal across the edge (horizontal axis is in pixels) yields a spatial resolution of 2 μm. (Bottom Right): Underwater image of an array of gold dots on the surface of silicon. During the scan, water was removed, resulting in loss of spatial resolution (central white patch). Reintroduction of water restored the contrast and spatial resolution.

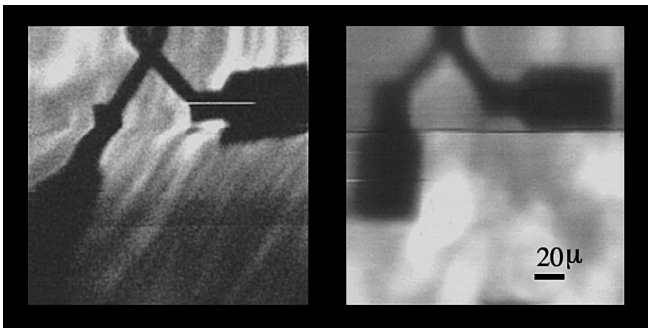

Fig. 6. Underwater image of a metal pattern taken at two different wavelengths. (Left) Image acquired at a wavelength of 6.25 μm. (Right) Image acquired of the same sample with the same probe and probe-to-sample height, at a wavelength of 5.14 μm. Note that the spatial resolution at the shorter wavelength is actually worse than the resolution at the absorption peak at water.

water (Fig. 2). The FEL wavelength was then changed to 5.14 μm, away from the peak and a second image was obtained without changing the sample or SNIM setup. It can be seen that the spatial resolution in the second image, taken at a shorter wavelength, is worse than in the first.

3. Infrared images of single living cells

Infrared images were obtained of single living fibroblasts. Fibroblasts are cells that are involved in a variety of repair processes in the body, such as wound healing. These cells secrete fibrinogen and can further change into other cells that specialize in making collagen, or into adipocytes for storing fat. Fibroblasts serve as models for studying cell motility [17]. Fig. 7 shows a phase contrast optical image of human fibroblasts. The cells have thinned out and spread across the substrate, generating very thin (~1 μm thick) extensions called filopodia or lamellopodia. Cell motion occurs in the direction of the extensions, as shown schematically in Fig. 8. The use of a tapered probe to obtain images allows us to localize molecules to specific features of the cell, such as the lamellopodium. Infrared images were obtained by tuning the FEL to both the amide absorption bands, and to the lipid absorption bands. Fig. 9 shows infrared images of human fibroblasts, with contrast provided by the intrinsic amide absorption bands characteristic of proteins. (Also shown for comparison are images of human hybridoma cells imaged at two wavelengths around 6 μm). Images were obtained of the

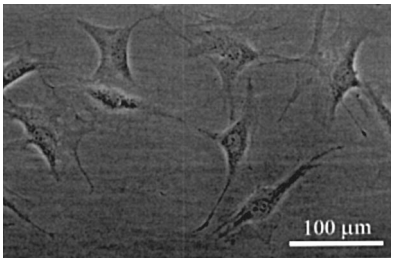

Fig. 7. Phase contrast microscope images of human fibroblasts [9].

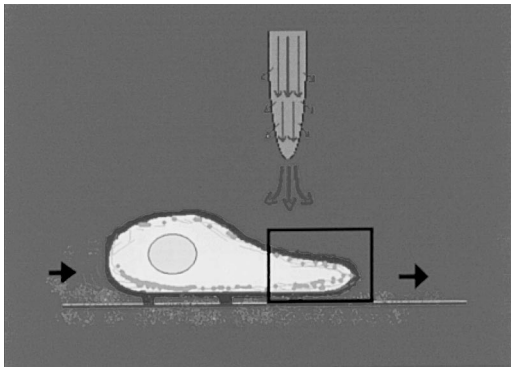

Fig. 8. Schematic diagram of a crawling cell, with the lamellopodium leading the cell body containing the nucleus. The distance between the cell surface and the probe, as well as the thickness of the lamellopodium, have been exaggerated for clarity.

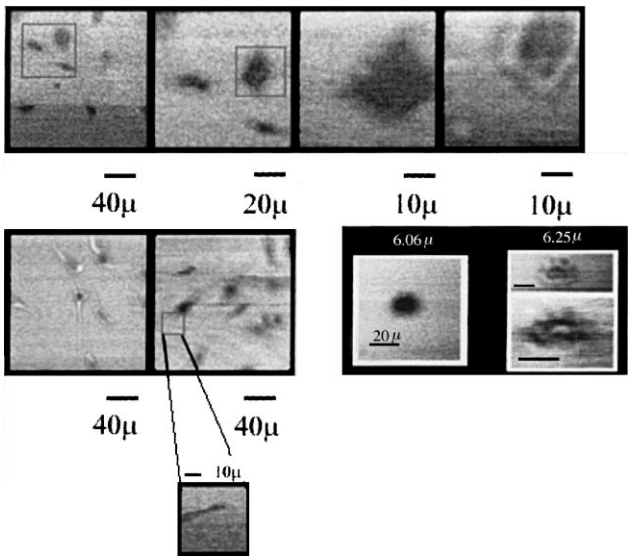

Fig. 9. (Top): Images of senescent fibroblasts at different wavelengths, and different magnifications. Images were acquired at 6.06 μm (amide I), and the image at the right was obtained at 6.25 μm. (Bottom Left): Images of crawling fibroblasts at a wavelength of 6.26 μm and at 6.45 μm (amide II), and a high resolution scan of the lamellopodium at the bottom, with the FEL tuned to the lipid peak at 5.76 μm, showing surprisingly high contrast. (Bottom Right): Image of a single human hybridoma cell at 6.06 μm, with the FEL tuned to the amide I absorption band, and to 6.25 μm, showing the variation in contrast in a different cell system.

lamellopodia with the FEL tuned to 5.76 μm, where the absorption is dominated by lipid molecules. What is surprising is that strong contrast is observed. The images in Fig. 9 were acquired with the shear force mechanism turned off, so that the height of the tip above the substrate was maintained. A ratio of the signal obtained through the lamellopodium with the signal obtained through buffer provides an estimate of the absorption of $(5.6 \pm 0.5) \times 10^{-2}$ OD at this wavelength. The absorption cross-section due to the C–O bond has been measured in standard lipid quantitation studies and is about 3×10^{-19} cm^2. Not all lipid molecules exhibit this absorption band, and some proteins with carboxylic acid groups in the side chains can also have some absorption cross-section, but these secondary contributions are generally negligible. This band has been used for quantitating fatty acids, trigylycerides and ester-linked phospholipids. One small point is that the absorption in this band is an estimate of the total concentration of acyl tails in lipid molecules. Most phospholipids have two or more tails. The composition of lipid molecules in the cell membrane exhibits a complex profile, with combinations of phospholipids, fatty acids and triglycerides. Until more is known about the detailed biochemistry and lipid composition in living cells, the estimates of lipid concentration based on absorption studies may vary by a factor of 2. Even with such a large potential source of systematic error, the observed absorption is between 250 and 500 times what one would expect from a single membrane bilayer.

3.1. Potential artifacts

Perhaps the most important potential artifact is inherent in using the near-field technique for quantitative spectroscopy. The extinction coefficients measured using far-field FTIR techniques cannot be used in order to assess the concentration of biomolecules, especially if there is significant coupling of longitudinal modes. In order to test whether the unusual coupling inherent in near-field techniques can lead to a several hundred-fold enhancement in the absorption cross-section [18], sections of atherosclerotic tissue were taken using a cryomicrotome, and the absorption was measured

using both near-field microscopy and FTIR studies of lipid deposits. No evidence of such an unusual enhancement of the cross-section was observed, either in the dry state or in the presence of water.

4. Cell motility

There are several different models of cell motility. The so-called "membrane flow" hypothesis was first postulated to explain the phenomenon of capping [19]. In this model, the cell membrane undergoes a cycle of polarized endocytosis, in which small pieces of the cell membrane in the trailing edge of the cell break away to form small vesicles. The resulting vesicles from this topological transformation are transported to the leading edge of the motile cell, thought to be the site of exocytosis. The alternative "rake" model [20], which is more widely accepted, suggests that polymerization of actin at the leading edge, and depolymerization at the trailing edge, lead to a "pull" on the membrane surface. The membrane is transported primarily along the cell surface, without any change in the topology of the cell. Actin is known to undergo polarized cycles of polymerization. Fluorescent labels are often used in attempts to distinguish between these models, in combination with specific mutations or the effects of drugs. There is interest in developing methods that do not require perturbing stains or labels capable of testing predictions that the two models have provided. One difference between the two models is that in the first case, the lamellopodium contains vesicles, whereas in the second model, relatively few vesicles are present in the cytoplasm. Because the presence of excess lipid molecules associated with these vesicles is expected to lead to increased absorption at wavelengths characteristic of the normal modes of lipid molecules, infrared microspectroscopy is particularly suited to testing these two models.

The absorbance change is given by $2.303N\sigma h$, where σ is the absorption cross-section, h the sample thickness and N the number of absorbers per unit volume. Let A_0 be the absorbance change due to a single bilayer of lipid. If the actual observed extinction is A_1, the ratio $\kappa = A_1/A_0$ provides a measure of the number of absorbing lipid molecules per unit volume, and as a test for the two leading models. Standard studies with glycerol trioleate have suggested that cross-section (per lipid tail) at 5.75 μm is around $\sigma = 3 \times 10^{-19}$ cm^2, giving an A_0 of about 1×10^{-4}. Lack of knowledge of the detailed lipid composition in the lamellopodia contributes to the uncertainty. The best estimates of the observed absorbance change range between an upper limit of about 500 times that from a single bilayer and the lowest limit of about 250.

For a lamellopodium in Fig. 8 in the absence of any internal vesicles, organelles or ripples on the cell surface, the absorption due to the cell membrane (and associated smooth inner membrane) is expected to be of the order of $4A_0$. Even with significant uncertainties, it appears that any model that does not require a large amount of lipid inside the lamellopodium predicts an absorbance that is several orders of magnitude too small.

Turning to models which do predict a large amount of lipid inside the cell extension, when the lamellopodium is filled with vesicles, the ratio is expected to increase because of the concentration c of vesicles, to $\kappa = 1 + \frac{1}{2}cS_l h$, where the thickness of the lamellopdium is $h \sim 1$ μm, the surface area of the vesicle is S_l ($\sim 10^{-11}$ cm^2 for spherical vesicles with $\sim$10 nm diameter). An enhancement in κ by a factor of about 250 is possible if the concentration c is about 10^{17} vesicles per cm^3. This rather high concentration corresponds to a value that is only about an order of magnitude less than the lipid concentration in neat lipid. This is surprising, and suggests that the vesicles are not far from being close-packed inside the lamellopodium. Further morphological studies would help to clarify the geometric shape of the vesicles, but at least enhancement of this magnitude is possible in this class of models.

Several enhancements of the two main models can be considered. One idea suggests that the lamellopodium is filled with endoplasmic reticulum that is folded back on itself many times. Membrane transport occurs via vesicles that fuse with the folded endoplasmic reticulum. This model is consistent with the absorbance change observed and also requires transport within the cell, and is a variant of the second membrane flow model. Our

data at present cannot distinguish between the endoplasmic reticulum and the cell membrane.

A variant of the "rake" model was suggested recently by Evans [21], and independently by Dokholyan [22]. In this model, the cell surface is highly rippled in the lamellopodium. One would expect an increase in lipid absorption while still confining the lipid molecules to the cell surface – there is then no need for vesicle formation or for transformations in cell topology. For a scanning tip of diameter L, and a sinusoidal ripple on the membrane surface of amplitude w and wavelength λ_r, detailed calculations [22] show that $\kappa = \sqrt{(1+a^2)}/b\, E(|b-\pi/2| \setminus \sin^{-1}(a/\sqrt{(1+a^2)})$, where $a = 2\pi w/\lambda_r$ and $b = 2\pi w/L$. Numerical estimates using the elliptic integral suggest that $b \sim 300$, $a \sim 300$ is needed for an enhancement in κ of about 250, which corresponds to an extremely rough surface indeed. Such a rough surface would have to be reconciled in some way with the presence of the polymerized actin network in the lamellopodium. Other surface morphologies, using rough surfaces that are not simply plane wave sinusoidal ripples, also suggest that small amplitude ripples cannot account for the observed enhancement. Models based on such a rough surface predict that the lateral diffusion rate of lipid molecules (measured by fluorescence studies) would have to be reduced greatly, by about a factor of 3. Such an enhancement has not been observed, although the question of the presence of ripples on the cell surface has not been settled.

The two alternative models were first proposed to explain the interesting phenomenon of capping [23]. Cap formation is restricted to motile cells, and models for cell capping have inspired the two different views of cell motility. Viewed as special cases of a much more general observation of polarized processes in single cells (such as early developmental processes in some oocytes), the potential for infrared spectroscopy to be able to study such processes appears to be of general value.

5. Conclusions

The extension of near-field techniques to underwater infrared imaging creates many problems, but also offers some advantages. We find that the spatial resolution achievable is actually enhanced by the presence of liquid water, with improved resolution being obtained at the peak of the absorption of the surrounding liquid. Because of the very low throughput of the tapered near-field probes, the use of increased laser power is desirable. The presence of water provides protection from thermal damage to the tapered fibers used, and images could be obtained at significantly higher laser power (~2 W) than has ever been demonstrated in near-field microscopy. Infrared FELs provide a unique source of tunable high-power radiation for this application.

The new underwater imaging technique was used to address a question of great interest in cell biology, concerning the mechanism of cell motion. Images were acquired of single living motile human fibroblasts with the FEL tuned to absorption bands characteristic of proteins, as well as absorption bands characteristic of lipid molecules. Our results suggest that the absorption due to lipid molecules in the lamellopodium is higher than that expected from the above surface membrane transport model of cell motility. These results may lend support to an idea that lipid molecules are involved in substantial topological or geometric membrane modifications associated with cell motility.

The new technique of underwater infrared microscopy has been shown to be promising. A recent report using the technique of apertureless imaging suggests that a spatial resolution of $\lambda/600$ may be achieved in near-field infrared microscopy [24]. The possibility of obtaining underwater infrared images with such enhanced resolution would mean that it is feasible to think of in situ vibrational spectroscopy at the macromolecular level.

Acknowledgements

Work supported in part by the National Science Foundation (DMR) and the Office of Naval Research (Contract No. N00014-94-1-1024). NVD acknowledges support from the NSF (CH 9728854) and the National Institutes for Health

(HG00989). S.E. acknowledges the receipt of a duPont Young Professor award. We thank S.J. Hong for advice on image analysis; D. Palanker for advice and help in AFM and fluorescence microscopy; Y.N. Jun, D. Fung, C. Smith, E. Evans for discussions; and the FEL center staff for their support and encouragement.

References

[1] F.S. Parker, Applications of Infrared, Raman, and Resonance Raman Spectroscopy in Biochemistry, Plenum, New York, 1983.
[2] D.R. Kodali, D.M. Small, J. Powell, K. Krishnan, Applied Spectroscopy 45 (1991) 1310.
[3] A.G. Jeung, Ph.D. Thesis, Stanford University, 1998.
[4] G.L. Carr, G.P. Williams, J.A. Reffner, Review of Scientific Instruments 66 (1995) 1643.
[5] N. Jamin, P. Dumas, J. Moncuit, W.H. Fridman, J.-L. Teillaud, G.L. Carr, G.P. Williams, Proc. SPIE 3153 (1997) 131.
[6] L.H. Kidder, I.W. Levin, E.J. Heilweil, Optics Letters 22 (1997) 742.
[7] M.K. Hong, A.G. Jeung, T.I. Smith, H.A. Schwettman, P. Huie, S. Erramilli, Third Free Electron Laser User's Workshop, Rome, 1996.
[8] M.K. Hong, A.G. Jeung, S. Erramilli, First Free Electron Laser User's Workshop, Stanford, 1994.
[9] M.K. Hong, A.G. Jeung, S. Erramilli, Second Free Electron Laser User's Workshop, New York, 1995.
[10] M.K. Hong, S. Erramilli, P. Huie, G. James, A. Jeung, Proc. SPIE 2863 (1996) 54.
[11] D.W. Pohl, W. Denk, M. Lanz, Applied Physics Letters 44 (1992) 651.
[12] E. Betzig, P.L. Finn, J.S. Weiner, Applied Physics Letters 60 (1992) 2484.
[13] P.J. Moyer, S.B. Kammer, Applied Physics Letters 68 (1996) 3380.
[14] D. Palanker, in preparation.
[15] H.A. Schwettman, T.I. Smith, R.L. Swent, Nucl. Instr. and Meth. A 341 (1994) ABS19.
[16] Y.N. Jun, D. Palanker, in preparation.
[17] R. Bellairs, A. Curtis, G. Dunn (Eds.), Cell Behaviour, Cambridge University Press, Cambridge, MA, 1982.
[18] A.G. Jeung, P. Huie, S. Erramilli, M.K. Hong, T.I. Smith, Proc. SPIE 3153 (1997) 115.
[19] M.S. Bretscher, Science 224 (1984) 681.
[20] M.S. Bretscher, Cell 87 (1996) 601.
[21] E. Evans, private communication.
[22] N.V. Dokholyan, Boston University Technical Report, 1998.
[23] R.B. Taylor, W.P.H. Duffus, M.C. Raff, S. de Patris, Nature New Biol. 233 (1971) 225.
[24] A. Lahrech, R. Bachelot, P. Gleyzes, A.C. Boccara, Optics Letters 21 (1996) 1315.